Proc. of the Second Intl. Conf. on Advances in Computing, Electronics and Electrical Technology - CEET 2014.

ISBN: 978-1-63248-034-7 doi: 10.15224/ 978-1-63248-034-7-98

A Method for 3D Reconstruction of ISAR Images Using Impulse-Radio UWB

Jiwoong Yu and Min-Ho Ka

***Abstract*—Recently, the use of Ultra Wide Band (UWB) technology has been increasing. This technology makes it possible to obtain high-resolution images of distant objects using microwave signals. A 2D ISAR algorithm was developed for defense and tomography and is used in medical approach. In this paper, the tomography algorithm is studied, using microwave similar to those used in reflection tomography. Three-dimensional images were reconstructed using two receiver antennae and one transmitter. The ISAR interferometry configuration was designed as a backprojection algorithm. When compared to 2D imaging, the signal has an elliptical range profile in the 3D observation mode. An elliptical range migration is confirmed in both theoretical and experimental results.**

***Keywords*— impulse radio UWB, ISAR image, 3D reconstruction, backprojection**

I. Introduction

In the past decade, UWB technology has been developed [1-11] with a bandwidth from 500MHz up [2-3]. This characteristic makes it possible to obtain high-resolution images of distant objects using microwave signals [4-7]. One of UWB technology can generate an impulse-radio pulse [1, 4-7], in a short time. These features allow for the reconstruction of quality images, and when using a short pulse, coupling interference and the multipath effect are absent.

Inverse Synthetic Aperture Radar (ISAR) is a powerful tool for imaging moving targets. ISAR 2D images are constructed from the scattered field of a target using its various sights and delay history [13]. Creating different views is simple when using a turntable that can be rotated to the required angle [6-8]. In this fixed geometry, back-projection tomography can be used for image reconstruction. Various studies have been conducted on reconstructing 2D images by using microwave signals [9-12], because these images are projected on rotating plane. Three-dimensional images not only require a projected image but also height information. The current methods of reconstructing 3D images require C-scans to be performed [11], which are physically bulky and time-consuming.

Jiwoong Yu

School of Integrated Technology, Yonsei Institute of Convergence Technology, Yonsei University
Republic of Korea

Min-Ho Ka
School of Integrated Technology, Yonsei Institute of Convergence Technology, Yonsei University
Republic of Korea

In general, the reconstruction of 3D images uses a separate receiver for different angles of the rotating plane. A baseline distance between each receiver can be obtained by adding a dimension [9-10]. If the receiver and the transmitter antennae are projected on a 2D, X-Y plane, then 3D information is estimated from data that is obtained by a separate receiver with a Z axis. The conceptual method of operation to calculate the height of objects is similar to the geometric configuration of delay in the Doppler radar, which is an interferometry altimeter radar able to detect landscape elevation from angle estimation [12].

The objective of this study is to reconstruct 3D images from additional receivers along the Z-axis and to develop a reconstruction signal processing algorithm.

In section 2, a wave model, geometric configuration of equipment and backprojection algorithm, which is a tomography method of obtaining 2D images, are presented. In section 3, the estimation of height is introduced. In section 4, experiment results are discussed, followed by concluding remarks in section 5.

II. Geometry

A. *Wave Propagation*

If the distance between the antennae and the object is far enough, it can be assumed that received and transmitted signals are parallel beam waves. A short pulse model that transmits signals looks like the delta function in (1).

$$s(t) = \delta(t - \tau) \tag{1}$$

The relation between round trip flight time and range is defined in (2).

$$r = c\tau/2 \tag{2}$$

B. *Geometric Configuration*

In 2D ISAR, the transmission antenna is assumed to be placed close to the receiving antenna, and the object to be far more than Fresnel region from the antennae on the turn table.

Proc. of the Second Intl. Conf. on Advances in Computing, Electronics and Electrical Technology - CEET 2014.

ISBN: 978-1-63248-034-7 doi: 10.15224/ 978-1-63248-034-7-98

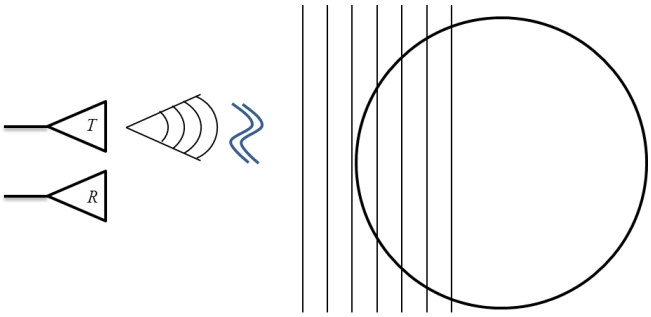

Figure 1. Transmitted signals and antenna configuration

The range, which is the distance between the antenna and object, can be calculated using the law of cosine as shown in (3)

$$r(\theta) = \sqrt{D^2 + R^2 - RD\cos(\theta_0 + \theta)} \tag{3}$$

where r is the distance between the antenna and the object, R is the distance between the center of rotation and the object, D is the distance between the center of rotation and the antenna, θ_0 is the initial angle of the object, and θ is the angle of rotation.

When using a parallel or plane wave, the range can be derived as in (4), which shows that received signals can be modeled by a set of lines like those in Figure 1. The geometric model is shown as Figure 2.

$$\begin{aligned} r(\theta) &= D + R\cos(\theta_0 + \theta) \\ &= D + R\cos\theta_0\cos\theta - R\sin\theta_0\sin\theta \\ &= D + x\cos\theta - y\sin\theta \end{aligned} \tag{4}$$

To prove theoretical range migration by slant viewing angle, the ISAR radar system with short pulse UWB radar was used. Figure 3 shows the system configuration. The target on the turn table is rotated with a motion controller.

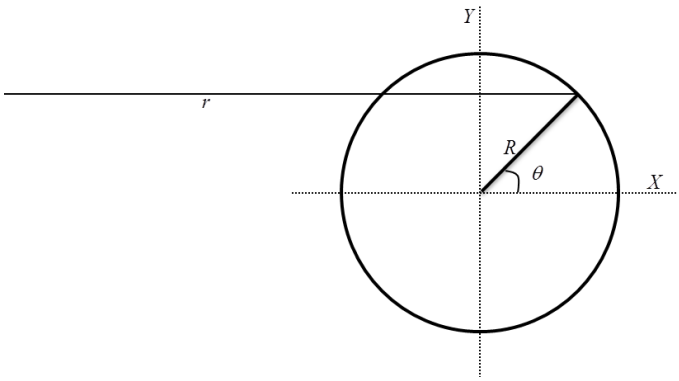

Figure 2. Geometric model of turning motion

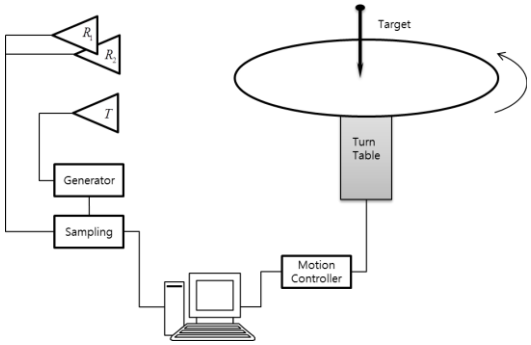

Figure 3. ISAR system configuration

C. *Backprojection*

The backprojection algorithm is used to make 2D images from received data [13], [14]. As shown in Figure 1, received signals are given by the sum of scattering on the lines. Equation (5) gives the projection of scattering along an arbitrary line of the X-Y plane, and f(x,y) refers to the image or real target.

$$g(\rho,\theta) = \int_{-\infty}^{\infty}\int_{-\infty}^{\infty} f(x,y)\delta(x\cos\theta + y\sin\theta - \rho)dxdy \tag{5}$$

Before reconstructing an image, a 2D inverse Fourier transform of F(u,v) is given by (6).

$$f(x,y) = \int_{-\infty}^{\infty}\int_{-\infty}^{\infty} F(u,v)e^{j2\pi(ux+vy)}dudv \tag{6}$$

The 1D Fourier transform of the received signal is s(t), with respect to time, and the angle is defined in (7).

$$S_\theta(w) = \int_{-\infty}^{\infty} s(t)e^{-j2\pi wt}dt \tag{7}$$

According to the Fourier slice theorem, F(u,v) has a symmetric property, and f(x,y) can be expressed by the 2D inverse Fourier transform with polar coordinates, as below (8).

$$f(x,y) = \int_0^{\pi}[\int_{-\infty}^{\infty} F(w,\theta)|w|e^{j2\pi wt}dw]d\theta \tag{8}$$

In practice, the Hamming or Hanning window can be used instead of the ramp filter |w|. This substitution was defined

Proc. of the Second Intl. Conf. on Advances in Computing, Electronics and Electrical Technology - CEET 2014.

ISBN: 978-1-63248-034-7 doi: 10.15224/ 978-1-63248-034-7-98

previously in (8), and the 1D Fourier transform of the received signal is shown in (9) using an independent angle and time.

$$f(x,y)=\int_0^{\pi}[\int_{-\infty}^{\infty} S_\theta(w)\,|w|\,e^{j2\pi wt}dw]d\theta \tag{9}$$

The filtered signal of this angle is Q_θ and is expressed by the following (10).

$$Q_\theta(t)=\int_{-\infty}^{\infty} S_\theta(w)\,|w|\,e^{j2\pi wt}dw \tag{10}$$

The image can be calculated by (11)

$$f(x,y)=\int_0^{\pi} Q_\theta(x\cos\theta+y\sin\theta)d\theta \tag{11}$$

where the equation (11) means that integrals along the lines of each angle of the filtering signal can become a reconstructed 2D image.

III. Estimation of Height

To acquire height information, both the general 2D ISAR and a different view of the 2D ISAR need to be observed. If we look at the circle of the trajectory of a point target from a higher or lower angle, the circle appears as an ellipse as shown in Figure 2. As the shadow of the circular ring looks like an ellipse, the inclined radar observes projected data on another plane, which means that the direction of the view is dependent on range.

The ellipse center is placed as the origin of the coordinate, and the Cartesian coordinate position is written by (12) and (13) where a is a semi-major axis and b is a semi-minor axis.

$$y=a\sin\theta \tag{12}$$

$$x=b\cos\theta \tag{13}$$

The transmitted signal is assumed to be a plane wave as in the following (14).

$$\begin{aligned} r(\theta) &= D'(z)+b\cos(\theta_0'+\theta) \\ &= D'(z)+b\cos\theta_0'\cos\theta-b\sin\theta_0'\sin\theta \\ &= D'(z)+x'\cos\theta'-\frac{b}{a}y'\sin\theta' \end{aligned} \tag{14}$$

The above equation (14) is slightly different compared with (4), where the height can be distinguished from the range equation. The modified range equation can be written by (15).

$$r(\theta)=D'(z)+x'\cos\theta'-\Delta Zy'\sin\theta' \tag{15}$$

The height can be calculated by eccentricity, b/a, and the distance between the center of the ellipse and the antenna. Height is proportional to ysinθ. Before estimating height, eccentricity or the viewing angle must be known.

IV. Results

The radar system is summarized in TABLE 1. Theoretical resolution of the used short pulse corresponds to 1mm. A short pulse generator requires a high-speed sampling convertor, and the equipment used in this study satisfies this criterion. The chosen angle step is 1 degree and every angle was observed.

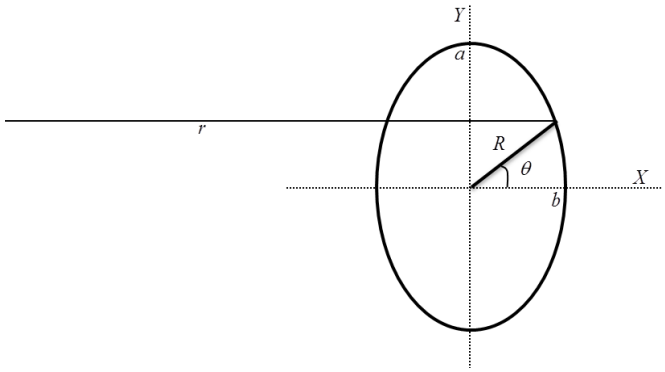

Figure 4. Geometrical model of the inclined view of a circular motion.

The observational results from the side view and slant view are shown in Figures 5 and 6. The object used was a 2.5 cm long needle. In Figure 6, the range profile has different flattening and range movement decreased, when compared to Figure 5. Figure 6 also has eccentricity.

TABLE I. RADAR PARAMETERS

PRF	1MHz
Pulse Width	~30 pico seconds
Number of Average Pulses	128
Sampling Interval	3/1024 nano seconds
Number of Samples	1024
Rotation Angle Step	1 degree
Rotation	1~360 degrees

Proc. of the Second Intl. Conf. on Advances in Computing, Electronics and Electrical Technology - CEET 2014.

ISBN: 978-1-63248-034-7 doi: 10.15224/ 978-1-63248-034-7-98

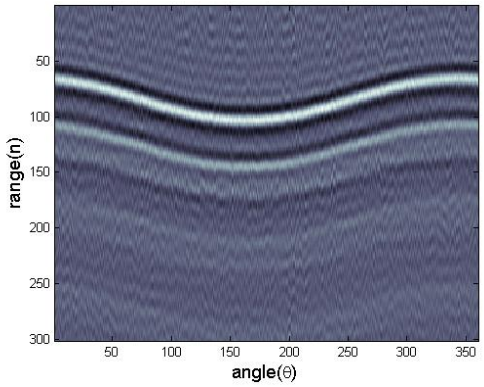

Figure 5. Side view of sinogram.

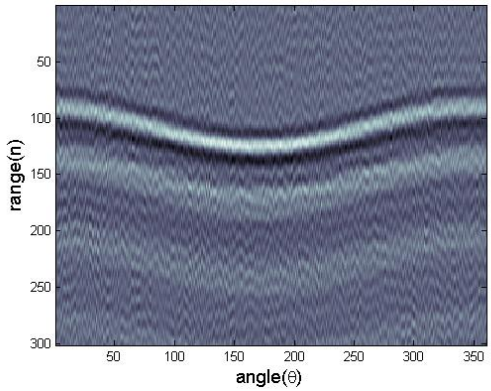

Figure 6. Inclined view of sinogram.

v. Conclusions

The 2D ISAR imaging algorithm for tomography was introduced in this research, which concentrated on reconstructing 3D images using two different viewing receivers. ISAR interferometry configuration is designed for reconstructing 3D image. In the 3D observation mode, the signal has an elliptical range profile. The short pulse UWB radar was used to ensure that the experiments performed without anechoic chamber conformed to those done anywhere. The results of this research suggest a new methodology for the configuration of observation. In future studies, resolution and analysis should be improved, and a focused algorithm and polar format interpolation of tomography developed.

Acknowledgment

This research was supported by the MSIP(Ministry of Science, ICT and Future Planning), Korea, under the “IT Consilience Creative Program” (NIPA-2014-H0201-14-1001) supervised by the NIPA(National IT Industry Promotion Agency). The authors gratefully acknowledge the support from Electronic Warfare Research Center at Gwangju Institute of Science and Technology (GIST), originally funded by Defense Acquisition Program Administration (DAPA) and Agency for Defense Development (ADD).

References

[1] F.-C. Chen and W. C. Chew, "Time-domain ultra-wideband microwave imaging radar system," in Instrumentation and Measurement Technology Conference, 1998. IMTC/98. Conference Proceedings. IEEE, 1998, pp. 648-650.

[2] M. Guardiola Garcia, L. Jofre Roca, and J. Romeu Robert, "3D UWB tomography for medical imaging applications," 2011.

[3] M. Guardiola, S. Capdevila, S. Blanch, J. Romeu, and L. Jofre, "UWB high-contrast robust tomographic imaging for medical applications," Electromagnetics in Advanced Applications, pp. 560-563, 2009.

[4] B. Levitas, "UWB Time Domain Measurements," in Antennas and Propagation, 2007. EuCAP 2007. The Second European Conference on, 2007, pp. 1-8.

[5] B. Levitas, "UWB time domain measurements," 2007.

[6] B. Levitas and J. Matuzas, "UWB radar high resolution ISAR imaging," in Second International Workshop Ultrawideband and Ultrashort Impulse Signals, 2004, pp. 228-230.

[7] B. Levitas and J. Matuzas, "Evaluation of UWB ISAR image resolution," in Radar Conference, 2005. EURAD 2005. European, 2005, pp. 89-91.

[8] L. Jofre, A. Broquetas, J. Romeu, S. Blanch, A. P. Toda, X. Fabregas, et al., "UWB tomographic radar imaging of penetrable and impenetrable objects," Proceedings of the IEEE, vol. 97, pp. 451-464, 2009.

[9] T. Sakamoto, "A fast algorithm for 3-dimensional imaging with UWB pulse radar systems," IEICE transactions on communications, vol. 90, pp. 636-644, 2007.

[10] B. Harker, A. Chadwick, and G. Harris, "Ultra-wideband 3-dimensional imaging (uwb 3d imaging)," Roke Manor Research Limited, UK, 2008.

[11] C. Özdemir, Inverse synthetic aperture radar imaging with MATLAB. Hoboken, NJ: Hoboken, NJ : Wiley, 2012.

[12] R. K. Raney, "The delay/Doppler radar altimeter," Geoscience and Remote Sensing, IEEE Transactions on, vol. 36, pp. 1578-1588, 1998.

[13] R. E. Woods and R. C. Gonzalez, Digital image processing. Upper Saddle River, NJ: Upper Saddle River, NJ : Person/Prentice Hall, 2010.

[14] A. C. Kak and M. Slaney, Principles of computerized tomographic imaging: Society for Industrial and Applied Mathematics, 2001.

About Author (s): Jiwoong Yu

Jiwoong Yu is a PhD candidate from the School of Integrated Technology at Yonsei University, Korea. He received his Master degree from the Department of Astronomy at Yonsei University, in 2011. His research focuses on SAR, ISAR, and signal processing.

About Author (s): Min-Ho Ka

Min-Ho Ka is a professor for the School of Integrated Technology at Yonsei University, Korea. He obtained his PhD at the Moscow Power Engineering Institute (MPEI), Russia, in Radar Engineering, in 1997. His current research activities focus on radar remote sensing and system design signals, as well as processing and image reconstruction.